Available online at www.sciencedirect.com
SCIENCE DIRECT®
Chemical Physics 292 (2003) 413–424
Chemical Physics
www.elsevier.com/locate/chemphys

Myoglobin in crowded solutions: structure and diffusion

S. Longeville[a,*], W. Doster[b], G. Kali[c]

[a] Laboratoire Léon Brillouin, CEA-CNRS, DSM-DRECAM, CEA Saclay, 91191 Gif-sur-Yvette, France
[b] Technische Universität München, Physik department e13, James Franck Strasse 1, D-85747 Garching, Germany
[c] Institut Laue-Langevin, 6 rue J. Horowitz, BP 156, F-38042 Grenoble Cedex, France

Received 20 December 2002; in final form 23 May 2003

Abstract

We present a neutron scattering study of the structure and diffusion of myoglobin solutions at high concentration. The protein–protein structure factor was determined by small angle neutron scattering (SANS) measurements using mean spherical analysis (MSA), and the intermediate scattering function was measured by neutron spin-scho spectroscopy. We observe the cross-over between self-diffusion at high Q and collective diffusion below the structure factor maximum. The self-diffusion coefficient decreases exponentially with concentration. The collective diffusion coefficient is shown to increase at low Q due to direct interactions.

Keywords: Myoglobin; Diffusion; Crowded solutions; Small angle neutron scattering; Neutron spin-echo

1. Introduction

Mainly due to the high concentration of proteins, the interior of biological cells is crowded with macromolecules whose volume fraction range up to 0.3. Under these conditions protein–protein interactions play a central role. In vivo, transient clusters of enzymes are formed depending on physiological requirements. A particular aspect concerns the transport of small molecules like oxygen by protein diffusion. The exchange of oxygen in the lung and in muscle cells is facilitated by macromolecular diffusion [1]. Red blood cells (RBC) are tightly packed with oxygen carrier hemoglobin. In the lungs hemoglobin binds O_2 and releases it in muscle cells, this hetero-association/dissociation must be done near the RBC membrane because of the very low solubility of oxygen. Consequently, the transport of oxygen depends on a delicate balance between two opposing factors: High protein concentrations, which will enhance the quantity of stored oxygen in the RBC, and crowding, which will depress the speed of oxygen binding (due to diffusion limited kinetics) because of strong protein interactions. In fact, an optimum concentration for the oxygen flux is observed [1]. Similarly, myoglobin is present at high concentration in muscle cells. It stores oxygen near the cell surface and is supposed to facilitate oxygen

* Corresponding author. Tel.: +33-(0)-1-69-08-75-30; fax: +33-(0)-1-69-08-82-61.
E-mail address: slongville@cea.fr (S. Longeville).

0301-0104/03/$ - see front matter © 2003 Elsevier Science B.V. All rights reserved.
doi:10.1016/S0301-0104(03)00292-1

transport to mitochondria by simple diffusion. One central goal of our project is to clarify the question, whether the mobility of different components in a living cell can be understood based on their intermolecular interactions. To this end we study the diffusion of myoglobin and hemoglobin molecules at high concentration. As a first step, we perform a structural analysis of the solution, based on SANS data (small angle neutron scattering) and the molecular form factor measured on dilute myoglobin solutions. As a result we obtain an estimate of the intermolecular structure factor, which is relevant to diffusion. In the second step we measure the time dependence of protein diffusion on the scale of the intermolecular distance using neutron spin-echo spectroscopy. Such a study provides insight into mechanistic aspects: How much is the diffusion coefficient depressed with concentration? How does the diffusion coefficient behave in the vicinity of the intermolecular structure factor maximum, where the interaction is most pronounced? Can we discriminate between short-time and long-time diffusion coefficient? How is hydrodynamic interaction between proteins affecting diffusion? Similar questions however on a different length scale were studied using dynamic light scattering (Photon Correlation Spectroscopy) first by Doherty and Benedek [2] on BSA, and later by Weissman et al. [3] and Weissmann and Marque [4]. Light scattering records the concentration fluctuations of over typical distances of few 1000 Å and requires optically transparent samples.

The paper is organised as follows: In Sections 2 and 3 we introduce the theoretical background generally used for structure and dynamics analysis by neutron scattering. Section 4 is devoted to experimental details and Sections 5 and 6 to the experimental results and analysis. Section 7 is devoted to discussion and conclusions are given in Section 8.

2. Theoretical background for SANS data analysis

The neutron intensity scattered by a solution of monodisperse spherical macromolecules is given by

$$I(Q) = (A * F(Q) * S(Q) + B) \otimes R(Q), \tag{1}$$

where A is an amplitude factor, B is a "background", $F(Q)$ is the normalised molecular form factor and $S(Q)$ the structure factor of the macromolecules. $R(Q)$ denotes the resolution function of the diffractometer and $\otimes$ refers to the convolution product.

2.1. The amplitude factor A

For a solution of spherical macromolecules, A depends on the volume fraction Φ, the specific volume v_0 of the macromolecules ($\Phi = v_0 C[\mathrm{mM}] \cdot N_a$), and the difference in the coherent scattering length densities between protein and solvent $(\Delta\rho)^2$ in cm^{-2} (see for example [5]), with N_a is the Avogadro number

$$A = \Phi v_0 (\Delta\rho)^2. \tag{2}$$

The experiments are performed on D-exchanged myoglobin in D_2O solutions, in order to maximise the contrast between the molecules and the solvent. The scattering length density for D_2O is obtained from

$$\bar{\rho}_s = \frac{d(T)}{M} N_a (2b_D^c + b_O^c), \tag{3}$$

where b_O^c is the coherent scattering length of oxygen, b_D^c of deuterium. Following Ref. [6] the density of D_2O at $T = 37$ °C amounts to $\simeq 1.099$ g cm^{-3}. It then follows for D_2O

$$\bar{\rho}_s = 6.327 \times 10^{10}\ \mathrm{cm}^{-2}.$$

The coherent scattering length density for protein molecules can be defined as

$$\bar{\rho}_p = \frac{\sum_i b_i^c}{v_p}$$

for fully protonated myoglobin one obtains

$$\bar{\rho}_p = 1.852 \times 10^{10}\ \mathrm{cm}^{-2}.$$

However in reality only a fraction of the labile protons exchanges with the deuterons of the solvent. Assuming that N_H denotes the total number of hydrogen atoms and f is the fraction of exchanged protons of the protein (fN_H deuterium on the protein, assumed to be homogeneously distributed) one finally can write

$$(\bar{\Delta}\rho)^2 = \left(\frac{\sum_{i\neq H} b_i^{\mathrm{c}} + fN_{\mathrm{H}} b_{\mathrm{D}}^{\mathrm{c}} + (1-f)N_{\mathrm{H}} b_{\mathrm{H}}^{\mathrm{c}}}{\bar{v}_{\mathrm{p}}} - \rho_{\mathrm{s}} \right)^2. \tag{4}$$

2.2. The background contribution B

The background contribution includes the incoherent scattering from both the solvent and the protein molecules, as well as the low angle contribution of the coherent scattering of D_2O. The latter is supposed to be constant within the accessible Q-range of the experiment. It is thus possible to extrapolate the solvent contribution of the solvent to infinite dilution. The incoherent scattering arises from the hydrogens, the deuterium and the nitrogen atoms of the protein molecules. This contribution can be written as

$$B = (1-\Phi)I^S(0) + \rho\left(n_{\mathrm{N}} b_{\mathrm{N}}^{\mathrm{i}^2} + fNb_{\mathrm{D}}^{\mathrm{i}^2} + (1-f)Nb_{\mathrm{H}}^{\mathrm{i}^2} \right), \tag{5}$$

where n_{N} denotes the number of nitrogen atoms per molecule, b^{i} refer to incoherent scattering lengths. We assume that the exchanged proton atoms have been removed from the solvent by successive dialysis. $I^S(0)$ includes incoherent and coherent contributions from the solvent.

2.3. Molecular form factor of myoglobin in solution

The normalised coherent molecular form factor can be written as

$$F(Q) = \frac{1}{\sum_{i,j} b_i^{\mathrm{c}} b_j^{\mathrm{c}}} \left\langle \sum_{i,j} b_i^{\mathrm{c}} b_j^{\mathrm{c}} \mathrm{e}^{-\mathrm{i}\mathbf{Q}\cdot\mathbf{r}_{ij}} \right\rangle \tag{6}$$

the bracket corresponds to the average over all equiprobable molecular orientations, b_i to coherent scattering lengths. Finally we get

$$F(Q) = \frac{1}{\sum_{i,j} b_i^{\mathrm{c}} b_j^{\mathrm{c}}} \sum_{i,j} b_i^{\mathrm{c}} b_j^{\mathrm{c}} \frac{\sin(Q\cdot r_{ij})}{Q\cdot r_{ij}}. \tag{7}$$

Assuming a spherical shape for myoglobin, then the form factor is given by the classical equation [7]

$$F(Q) = \left[\frac{3}{(Q\cdot R)^3} (\sin(Q\cdot R) - Q\cdot R\cos(Q\cdot R)) \right]^2. \tag{8}$$

The radius R corresponds to the exact radius of the sphere and is related to the radius of gyration by the formula $R_{\mathrm{g}}^2 = 3/5R^2$. The radius of gyration is generally extracted from the measurements by the expansion of the form factor in the Guinier regime ($QR \ll 1$)

$$F(Q) \sim \mathrm{e}^{-\frac{1}{3}Q^2 * R_{\mathrm{g}}^2}. \tag{9}$$

2.4. The structure factor of concentrated protein solutions

The determination of the protein structure factor is performed via computation of the Ornstein–Zernike equations (OZE) relating the pair correlation function $h(r) = g(r) - 1$ to the direct correlation function $c(r)$

$$h(r) = c(r) + \frac{6}{\pi}\eta \int c(\mathbf{r}')\cdot \mathbf{h}(|\mathbf{r}-\mathbf{r}'|)\,\mathbf{d}^3\mathbf{r}. \tag{10}$$

In the reciprocal space the OZE can be written as

$$S(Q) = 1 + \hat{h}(Q) = \frac{1}{1-\hat{c}(Q)}, \tag{11}$$

where

$$\hat{c}(Q) = \rho \int_V c(r)\mathrm{e}^{-\mathrm{i}\mathbf{Q}\cdot\mathbf{r}}\,\mathbf{d}^3\mathbf{r}, \tag{12}$$

where $\rho = C[\mathrm{mM}]\cdot N_{\mathrm{a}} = \Phi/(4/3\pi\cdot R^3)$ is the number of molecules per unit volume due to the isotropy of the system

$$\hat{c}(Q) = \frac{24\Phi}{\sigma^3} \int_0^\infty c(r)\frac{\sin(Q\cdot r)}{Q}\cdot r\,\mathrm{d}r. \tag{13}$$

To solve the OZE equations one needs a closure relation. Different approximations have been developed in the preceding decades such as mean spherical approximation (MSA) or hypernetted chain approximation (HNC). For the first case (MSA) there is a direct and very simple relation between $c(r)$ and the pair-potential function $V_{ij}(r)$:

$$c(r) = -\beta V_{ij}(r) \quad \text{for } r > \sigma_0 \tag{14}$$

and

$$g(r) = 0 \quad \text{for } r < \sigma_0. \tag{15}$$

Although at least three types of charged species are present in solution, the macromolecule and the

positive and negative ions in the buffer, we treat the solution as a one-component system. This is reasonable because the relative scattering intensity of the solvent ions is negligible. The macromolecule is considered as surrounded by a dielectric continuum and the effect of the charges on the structure are taken into account via their modification of the inter-protein potential. They screen the electrostatic potential, this is the one component model (OCM) with Debye–Hückel approximation (DHA) (i.e: the Derjaguin–Landau–Vervey–Overbeek: DLVO potential – in its simplest form: Hard sphere with Yukawa tail) as defined by:

$$\beta V_{ij}(r) = +\infty \quad \text{for } r < \sigma_0, \tag{16}$$

$$\beta V_{ij}(r) = V_{ij}(\sigma_0)\sigma_0 \frac{e^{-\kappa(r-\sigma_0)}}{r} \quad \text{for } r > \sigma_0, \tag{17}$$

$$V_{ij}(\sigma_0) = \frac{Z_p^2 L_B}{(1+\kappa\sigma_0/2)^2}\frac{1}{\sigma_0}, \tag{18}$$

where $L_B = e^2/(4\pi\epsilon_0\epsilon kT)$ is the Bjerrum length (the minimum distance which can be supported between two charges in a solvent) $L_B \sim 7.5$ Å in H_2O at 25 °C and $L_B \sim 7.25$ Å in D_2O at 37 °C. ϵ is the relative dielectric constant $\varepsilon = 74.32$ in D_2O at 37 °C. σ_0 is the protein diameter. Z_p is the charge of the protein in unity of electron charge e. $\kappa = (4\pi L_B \Sigma_{i=1}\rho_i Z_i^2)^{1/2}$ is the inverse Debye screen length *due to small ions*. κ^{-1} has the dimension of a distance. For aqueous solution with added monovalent salt (NaCl)

$$\kappa^{-1}(\text{Å}) = L_D = \frac{8.13}{\sqrt{L_B(\text{Å})I(\text{mol l}^{-1})}}, \tag{19}$$

where I is the ionic strength of the solution

$$I = \frac{1}{2}\sum_i C_i(\text{mol l}^{-1})Z_i^2. \tag{20}$$

2.5. Algorithm for S(Q) data fitting

2.5.1. The analytical solution by Hayter and Penfold [8]

They computed analytically the solution of Eq. (10) with approximations (16)–(18).

For $r < \sigma_0$

$$c(x) = A + Bx + \frac{1}{2}\eta A x^3 + \frac{C\sinh(kx)}{x} + \frac{F(\cosh(kx)-1)}{x} \tag{21}$$

with $x = r\sigma_0$
for $r > \sigma_0$

$$c(x) = -\gamma\exp(-kx)/x. \tag{22}$$

This expression is given in reduced units but is quite similar to (17) and (18). Details on parameter A, B, C, F and γ are given in [8].

2.5.2. The correction method of [9]

The DLVO potential does not account for any dependence on the concentration, and this approximation is strictly valid only for $\Phi \to 0$. However, the ionic strength of the solution will increase with concentration of the macromolecules. In a paper by Belloni [9] a rescaling method is introduced which can directly be incorporated in the preceeding MSA algorithm of Hayter and Penfold [8]. In this generalised one component model (GOCM) the interaction potential for $r > \sigma_0$ remains of the Yukawa type with $\kappa = 1/L_D$ and L_D is the Debye length due to small ions. Only the prefactor, hence the contact potential is rescaled (Fig. 1).

$$\beta V_{ij}(r) = V_{ij}(\sigma_0)\sigma_0 \frac{e^{-\kappa(r-\sigma_0)}}{r} \quad \text{for } r > \sigma_0 \tag{23}$$

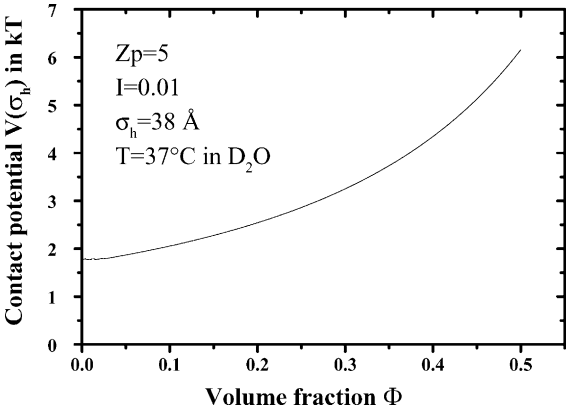

Fig. 1. Volume fraction dependence of the contact potential $V(\sigma_0)$ using the rescaling method of [9].

with

$$V_{ij}(\sigma_0) = Z_p^2 L_B X^2 \frac{e^{-\kappa\sigma_0}}{\sigma_0} \quad (24)$$

The parameter X^2 depends on the screening parameter κ and volume fraction Φ; it is calculated as follows

$$X = ch(\kappa\sigma_0/2) + U(\kappa\sigma_0/2ch(\kappa\sigma_0/2) - sh(\kappa\sigma_0/2)), \quad (25)$$

where

$$U = \frac{\mu}{(\kappa\sigma_0/2)^3} - \frac{\gamma}{\kappa\sigma_0/2} \quad (26)$$

and

$$\gamma = \frac{\Gamma\sigma_0/2 + \mu}{1 + \Gamma\sigma_0/2 + \mu}, \quad (27)$$

where Γ is found by solving numerically the MSA equation

$$\Gamma^2 = \kappa^2 + \frac{q_0^2}{(1 + \Gamma\sigma_0/2 + \mu)^2}, \quad (28)$$

where $\mu = 3\Phi/(1 - \Phi)$ and

$$q_0^2 = \frac{24Z^2e^2\Phi}{4\pi\varepsilon_0\varepsilon_r\sigma_0 kT}. \quad (29)$$

3. Theoretical background for NSE data analysis

Neutron spin-echo spectroscopy [10,11] measures the polarisation $P(Q,\tau)$ of the neutron beam scattered by a sample as a function of the wave vector Q and the Fourier time τ. To a first approximation, $P(Q,\tau)$ is equal to the intermediate scattering function of the system $I(Q,t) = S(Q,t)/S(Q)$. If the scattering process is coherent (favourable for NSE measurements) we obtain for a solution of macromolecules

$$S(Q,t) = \frac{1}{\rho}\sum_{i,j} |F(Q)|^2 \langle \exp(-iQ \cdot [r_i(0) - r_j(t)]) \rangle, \quad (30)$$

where ρ is the number density of protein per unit volume, $F(Q)$ the molecular form factor (non-normalised), $r_i(0)$ the position of protein i at time $t = 0$ and $r_j(t)$ of protein j at time t. From the intermediate scattering function one can define a generalised diffusion coefficient which is wave vector and time dependent

$$D(Q,t) = -\frac{1}{Q^2}\frac{\partial}{\partial t}\ln(I(Q,t)). \quad (31)$$

For such measurements $D(Q,t)$ is a collective diffusion coefficient, it is related to the decay of the pair correlation function.

4. Sample preparation and neutron scattering experiments

4.1. Sample preparation

Salt-free solutions were prepared from (horse heart) myoglobin (Sigma). A given amount of D-exchanged dry protein (g) per volume of solvent was dissolved in D_2O. The concentrations were then calculated using a specific volume of 0.74 cm^3 g^{-1} [12]. No salt was added.

4.2. SANS experiments

SANS measurements were made at the diffractometer PACE located on the cold source guide G1 of the Orphée reactor of the Laboratoire Léon Brillouin (CEA Saclay). The incident wavelength was set to $\lambda = 6.07$ Å with a wavelength spread of $\Delta\lambda/\lambda = 0.1$. In order to cover the full wave vector range corresponding to the relevant structure factor we used two configurations corresponding to two sample-detector distances $L_{SD}^1 = 0.768$ m and $L_{SD}^2 = 4.618$ m. The respective wave vector range were $Q = 0.04$–0.4 Å^{-1} and $Q = 0.0067$–0.071 Å^{-1}. The samples were 1 mm thick which correspond to transmission ~0.8. Six different solutions ranging from 6 mM up to 30 mM were studied at the physiological temperature $T = 37$ °C. The molecular form factor was measured on two solutions 0.25 and 0.5 mM. Since the differences in shape were limited to uncertainties of the measurements, we assume the forward scattering intensity as arising from $F(Q)$.

The spectra were corrected for background, empty cell and absorption by the standard procedure following [13], no solvent subtraction was performed prior to data analysis.

4.3. NSE experiments

Three neutron spin-echo spectrometers G_1bis and MESS of the LLB and IN15 of the ILL were used for measurements of the intermediate scattering function (ISF). We studied different solutions with myoglobin concentrations ranging from 5.2 to 35 mM. This corresponds to a volume fraction of $\Phi \sim 0.07$ up to $\Phi \sim 0.44$.

G_1bis is a, high flux, medium wave vector, mixed resonance-conventional spin-echo spectrometer [14,15]. We used incident wavelength of $\lambda = 10$ Å, with a Full Width Half-Maximum (FWHM) of the distribution of $\delta\lambda/\lambda = 0.13$. Measurements were performed without other collimations than the resonance coils windows corresponding approximately to $\gamma \sim 1.2°$. It was used in the wave vector range $Q \sim 0.05$–0.25 Å^{-1}. The Fourier time range was $\tau \sim 30$ ps–22 ns. MESS is a SANS NSE spectrometer, with a the distance sample to detector of $L_{SD} \sim 6$ m. The beam collimation is $\gamma \sim 0.5°$, which allows measurements down to $2\theta \sim 1°$. The maximum wavelength distribution was set to $\lambda \sim 6$ Å, with a full width half maximum $\delta\lambda/\lambda = 0.18$. The minimum wave vector of the measurement was $Q = 0.025$ Å^{-1}. IN15 is a long wavelength SANS NSE spectrometer located on the High Flux reactor of the Institut Laue Langevin. It takes advantage of the λ^3 dependence of the spin-echo time to reach very high times. Two wavelengths were used for the experiments, $\lambda \sim 9$ Å and $\lambda \sim 15$ Å to cover the full range of relevant wave vector to be compared with the other spectrometers. The maximum Fourier time was $\tau \sim 200$ ns. The full width half maximum of the incident wavelength distribution was set to $\delta\lambda/\lambda = 0.15$. The minimum wave vector of the measurement was $Q = 0.022$ Å^{-1}.

For all spin-echo experiments we used 30×40 mm^2 quartz cell of 1 mm thickness oriented perpendicular to the incident beam.

5. SANS results

The corrected spectra are shown on Fig. 2 in absolute intensities (cm^{-1}) for myoglobin concentrations ranging from 6 to 30 mM. We used a scaling factor to adjust the intensity of the small Q configuration to the high Q one, but the discrepancy remains smaller than 8%. The molecular form factor was measured in two dilute solutions of 0.25 and 0.5 mM. This corresponds, respectively, to volume fractions $\Phi \sim 3.1 \times 10^{-3}$ and $\Phi \sim 6.2 \times 10^{-3}$. The radius of gyration extracted from the Guinier regime was $R_g \sim 15.9$ Å, compatible with the value previously reported in the literature [16,17]. The measured myoglobin form factor is compared with the intra-molecular form factor refined from the crystallographic structure and compared to the form factor of a sphere (convoluted by instrumental resolution). The results of the refinements are shown on the Fig. 3 for myoglobin, the extracted radius of the protein is $R = 20.6$ Å. The results measured by SANS and deduced from X-ray scattering are comparable with a good degree of accuracy.

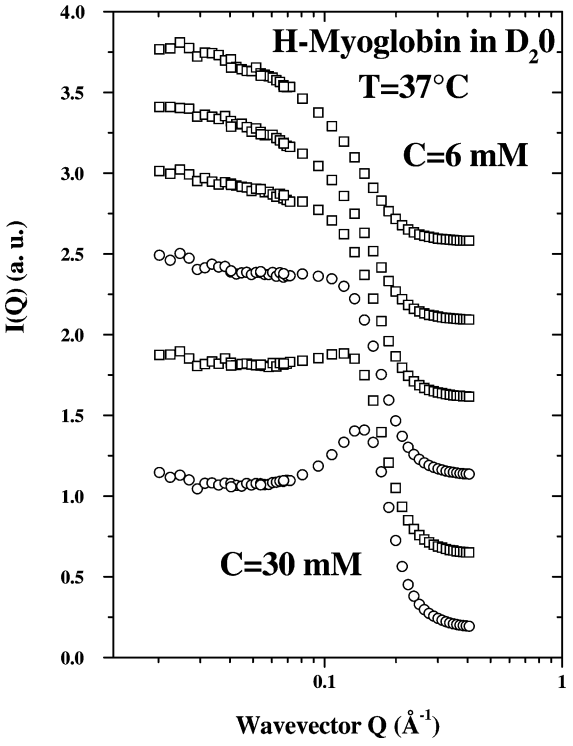

Fig. 2. Neutron scattering intensity $I(Q)$ measured from concentration myoglobin solutions at different concentrations: 6 mM (94 mg ml^{-1}), 10 mM (169 mg ml^{-1}), 15 mM (254 mg ml^{-1}), 20 mM (338 mg ml^{-1}), 25 mM (423 mg ml^{-1}) and 30 mM (508 mg ml^{-1}).

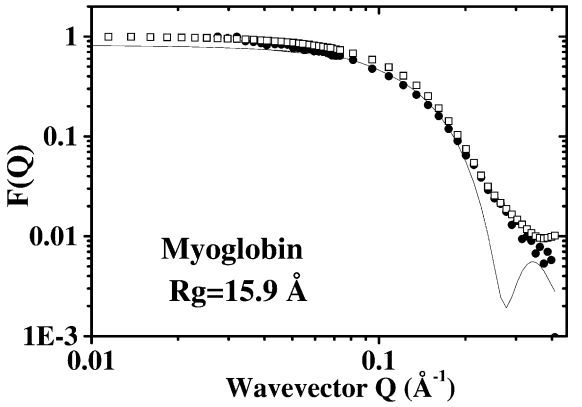

Fig. 3. Normalised form factor of myoglobin calculated from the PDB structure (open squares), measured experimentally on Mb solution of 0.25 mM (full circles) and compared to the form factor of a sphere convoluted by experimental resolution (full line), Eq. (8).

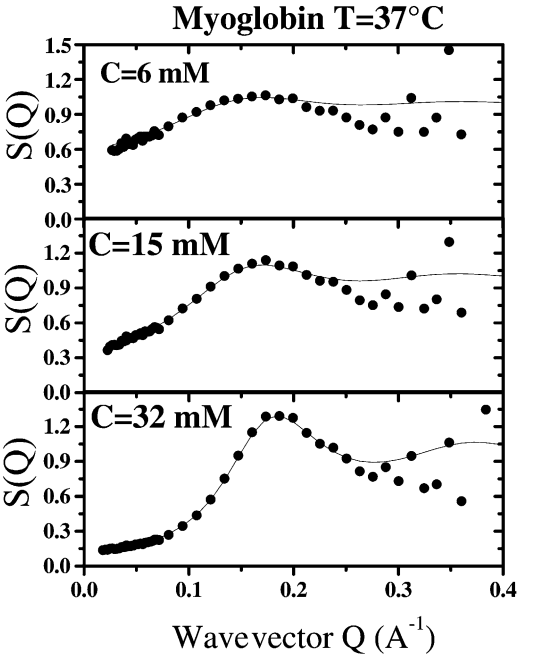

Fig. 4. Structure factor $S(Q)$ of myoglobin solutions ranging from 6 to 30 mM. The points are deduced from experiments and continuous lines the refinements using RMSA.

The refinements of the spectra were performed using the RMSA algorithm with the experimental molecular form factor of myoglobin. A contribution was added in order to account for an additional intensity at low wave vectors probably arising from small amount of aggregation. At high concentrations a maximum in $S(Q)$ emerges, due to intermolecular repulsive interactions. The results of the refinements are shown in Fig. 4, the points are the values of $S(Q)$ deduced from the SANS measurements and the continuous lines were deduced from the analytical formulae. Two parameters are relevant for the structure factor refinements, the radius of the protein and the absolute protein charge $|Z_p|$. The two other parameters are the amplitude factor and background intensity. They depend on the protein volume, on the protein concentration and the number of exchanged protein labile protons.

5.1. The amplitude factor A: Can we use it to compute the number of exchanged protons?

The amplitude factor A was refined using formulae (2) and (4), v_0 and Φ were computed from the protein diameter $\sigma_0 = 2R$ and concentration at each step of the refinement. We finally get $f \simeq 0.05 \pm 0.01$ for concentration ranges 6–30 mM. This corresponds approximately to 20% of labil protons which has been exchanged. However due to the necessity to introduce a factor for the superposition of the two configuration spectra, this value could be affected by significant systematic errors.

5.2. The background contribution B: Is it sensitive to the number of exchanged protons?

The background intensity was refined as a function of the concentration. The fraction of exchanged protons is found to be negligible. However, the maximum difference between fully exchanged and nonexchanged protein solution (only 257 protons can theoretically be exchanged) corresponds to $f = 0.21$ which induces a intensity difference of the order of 0.01 cm^{-1}. To measure with such a precision would require a very high statistics, and moreover at high D_2O fraction such an intensity difference can easily arise from the isotopic impurity of heavy water. It is thus very

difficult to extract any fraction of exchanged protons from the incoherent scattering intensity.

6. The neutron spin-echo results

The results obtained by neutron spin-echo spectroscopy are shown in Fig. 6 (G_1bis) [18] and Fig. 7 (IN15) for solute concentration of 14.7 and 30 mM. These values correspond to volume fraction of $\Phi \sim 0.2$ and $\Phi \sim 0.4$. For the range of wave vectors and concentration under investigation we could not detect in the time dependence of the intermediate scattering function any departure from the single exponential behaviour: The curves were refined using a stretched exponential function and the results concerning the stretching parameter indicate $\beta \simeq 1$. This needs to be verified for cases where the full decay of the intermediate scattering function is not observed. We corrected for λ^3 dependence of the spin-echo time by directly introducing the $D(Q) \cdot Q^2$ in $I(Q,t)$ as was previously described [18]. Such a definition should include all pair contribution but as was mentioned above we assumed that the coherent scattering length density between protein and solution are strong enough to neglect any contribution other than the protein–protein one (especially incoherent scattering). The results of the refinements are

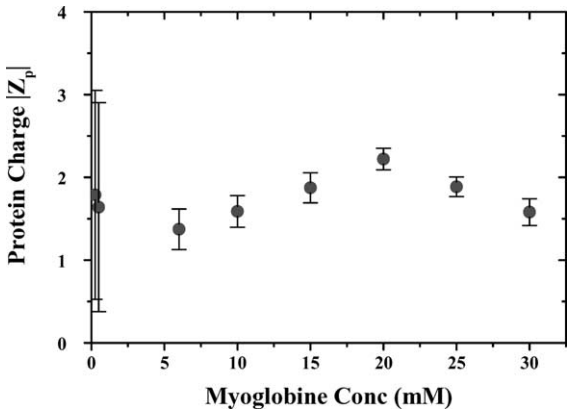

Fig. 5. Effective protein charge $|Z_p|$ obtained from RMSA analysis of myoglobin solutions with concentrations ranging from 6 to 30 mM.

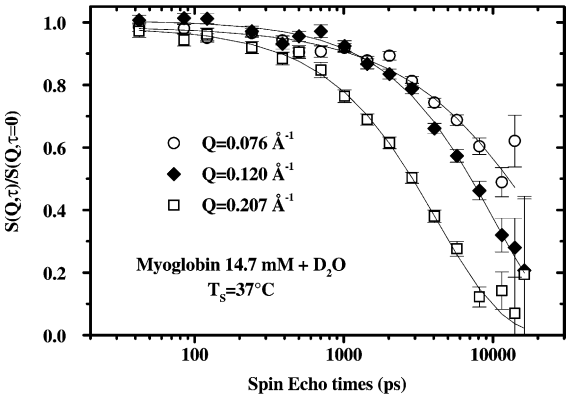

Fig. 6. Intermediate scattering function measured on the spin-echo spectrometer G_1bis for myoglobin solutions of 14.7 mM and three different wave vectors around the structure factor maximum.

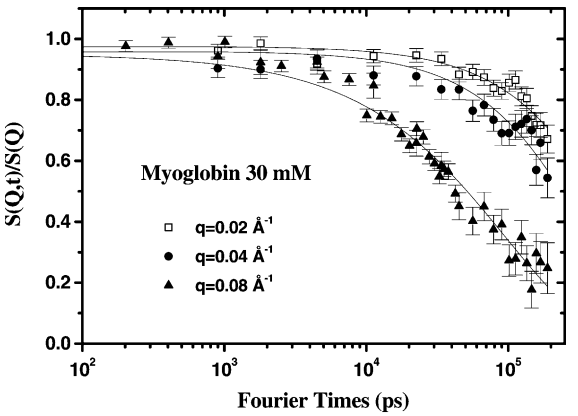

Fig. 7. Intermediate scattering function measured on the spin-echo spectrometer IN15 for myoglobin solutions of 30 mM and three different wave vectors.

shown of Fig. 8, $D(Q)$ was obtained with the 3 different spectrometers for different concentrations. For each protein volume fraction Φ the wave vector dependence of the apparent diffusion coefficient $D(Q)$ is always the same. $D(Q)$ tends to a plateau value D^{ϕ} at high wave vectors and increases at low wave vectors. D^{ϕ} is strongly volume fraction dependent as can be seen in Fig. 8 and was shown in more details on Fig. 5 of [18]. Due to the limited wave vector range of measurements ($Q > 0.025$ Å^{-1}) we were not able to verify that $D(Q)$ tend to a constant value at low wave vectors.

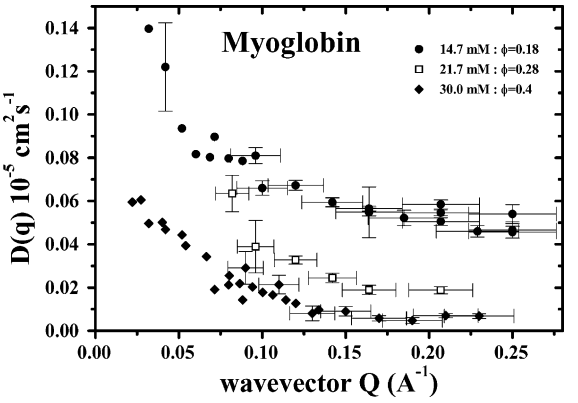

Fig. 8. Wave vector dependence of the apparent diffusion coefficient $D(Q)$ for three different myoglobin concentrations. One can observe a plateau at high Q, which is related to the self-diffusion coefficient $D(Q) \simeq D_s^{\phi}$, and the increase at low wave vector is due to the direct electrostatic interaction (see text).

7. Discussion

7.1. D^{ϕ}: the self-diffusion coefficient

According to the Figs. 4 and 8 the plateau in $D(Q)$ is observed in the regime of wave vectors corresponding approximately to $S(Q) \simeq 1$. In this regime the moment rule pointed out by de Gennes [19] for coherent neutron scattering in simple liquids is de-facto respected. The incoherent approximation of coherent neutron scattering postulated by Vineyard [20] is valid. In other terms, since $QR \gg 1$, a small modification of $\Delta r = r_i(0) - r_j(t)$ (i and j refer to proteins) induces a strong phase shift in the exponential term and thus the average over the nearest neighbours reduces the $i, j \neq i$ term in the scattering function to 0. This was also pointed out for light scattering experiments [21] on colloids. Thus for a solution of protein in D_2O, the intermediate scattering function measured by coherent neutron scattering reduces to

$$I^{c}(QR \gg 1, t) \simeq \langle \exp(-\mathrm{i}Q \cdot [r_i(0) - r_i(t)]) \rangle. \quad (32)$$

Hence, within a good approximation, D^{ϕ} is equivalent to the self-diffusion coefficient $D^{\phi} \simeq D_s$ which is generally deduced from neutron scattering measurements as the $Q = 0$ limit of incoherent scattering.

$$D^{\phi} = D^{c}_{QR \gg 1}(Q) \simeq D_s = \lim_{Q \to 0} D^{s}(Q). \quad (33)$$

We have reported previously the volume fraction dependence of D^{ϕ} [18]. It is consistent with the results obtained with macroscopic tracer diffusion techniques by previous authors [22] on myoglobin, but the concentration range of measurements was extended.

7.2. $D(Q)$: the apparent diffusion coefficient

As mentioned above $D(Q)$ measures the *collective* diffusion of the protein in solutions over distances $d \simeq 2\pi/Q$. Structural (direct interaction due to inter-particle potential) and hydrodynamic interactions (effect of the motions of a particle on others via solvent) are generally separated [23–25] using

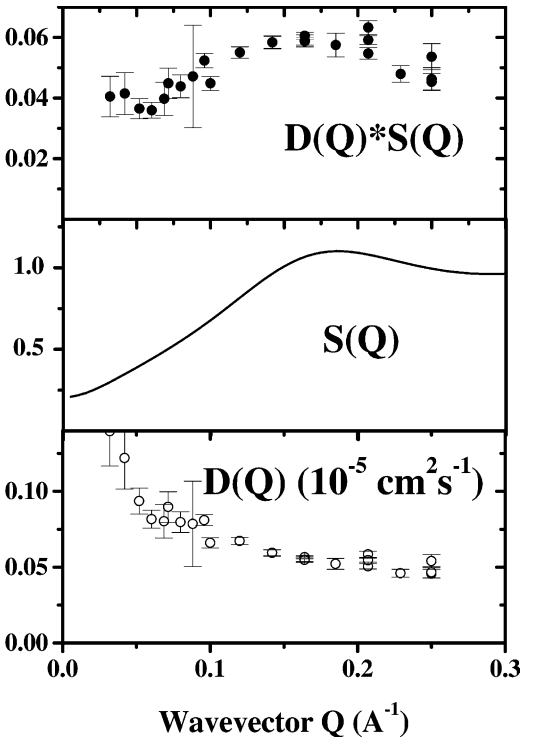

Fig. 9. Apparent diffusion coefficient $D(Q)$ deduced from NSE measurements (bottom), structure factor deduced from RMSA analysis (middle) and $S(Q) \cdot D(Q)$ for myoglobin solutions of 14.7 mM ($\Phi \sim 0.2$).

$$D(Q) = D_\infty \frac{H(Q)}{S(Q)}, \tag{34}$$

where D_∞ is the infinite dilution diffusion coefficient given by Stokes–Einstein relation: $D_\infty = kT/6\pi\eta R$ for a spherical particle. $H(Q)$ denotes the hydrodynamic factor. $H(Q) = 1$ if there is no hydrodynamic effects. We used the structure factor determined by the RMSA refinements and the measured $D(Q)$ to compute the product $D(Q)\cdot S(Q)$. It is presented on Figs. 9 and 10 for two different concentrations corresponding, respectively, to volume fractions $\Phi \simeq 0.2$ and $\Phi \simeq 0.4$. The top of Fig. 9 shows that the hydrodynamic factor is wave vector dependent for $\phi \sim 0.2$. It seems to oscillate in phase with the structure factor. For a given wave vector $H(Q)$ is very strongly protein volume fraction dependent. For a 30 mM solution of myoglobin (Fig. 10) the product $S(Q)\cdot D(Q)$ also seems to oscillate in phase with the structure factor although the results are very noisy. The magnitude of the error bar results from the incomplete decay measurement of the intermediate scattering function in the experimental time window. $I(Q,t)$ can not be measured down to $I(Q,t) \simeq 0$ for high concentration myoglobin solutions for small wave vectors on IN15 spectrometer, and over the full wave vector range for $G_1 bis$.

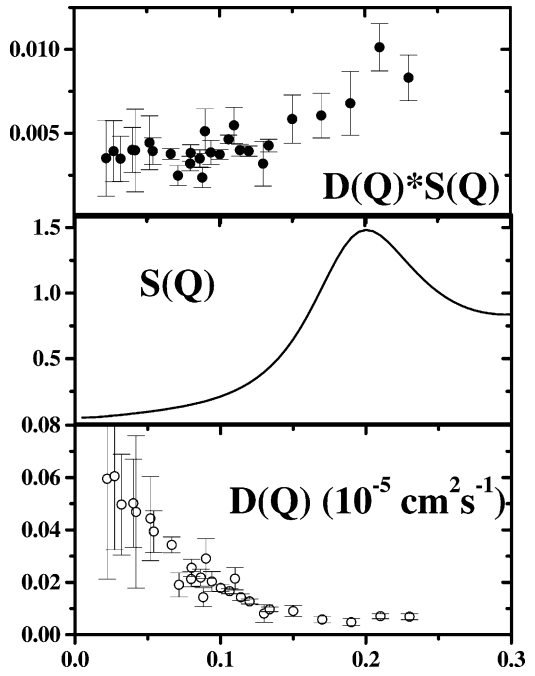

Fig. 10. Apparent diffusion coefficient $D(Q)$ deduced from NSE measurements (bottom), structure factor deduced from RMSA analysis (middle) and $S(Q)\cdot D(Q)$ for myoglobin solutions of 30 mM ($\Phi \sim 0.4$).

7.3. D^c: the collective diffusion coefficient

The apparent diffusion $D(Q)$ measured on protein solutions by DLS does not show any significant wave vector dependence [26]. This quantity has been interpreted as the concentration fluctuation relaxation, and is often related to the transport diffusion coefficient *when a protein concentration gradient is observed*. The characteristic distances probed by DLS (few 1000 Å are much larger than the one measured by NSE in this experiment (50 Å to few 100 Å) so due to the limited wave vector range of the measurements ($Q > 0.025$ Å^{-1}) we were not able to observe any plateau in $D(Q)$ at small wave vectors. One should nevertheless notice from the Fig. 9 that the lowest wave vector limit in $D(Q)$ seems to be less concentration dependent than the self-diffusion coefficient which agrees with previous observations based on different techniques [27].

8. Conclusion

We have performed static and dynamic neutron scattering measurements on myoglobin solutions to study the structure and diffusion processes as a function of the concentration. The structure seems correctly described by the RMSA refinements using a Yukawa type screened electrostatic potential, although the pD of the solution is near the isoelectric point of the protein (hence it carries a small charge), and no buffer was added to the solution to increase the protein charge. The radius of the protein deduced from RMSA analysis ($R \simeq 16$ Å) corresponds approximately to the value which can be deduced from SANS measurements ($R \simeq 17.3$ Å) [16]. The small discrepancy probably arises from the nonspherical shape of myoglobin and the repartition of

exchanged protons atoms near the protein surface. It is interesting to note that the myoglobin concentration deduced from the analysis is slightly lower than the one measured by other methods on our sample. Such an observation was previously reported by Krueger on hemoglobin in blood cells [28] and in solution [29]. It was interpreted by the authors as resulting from oligomer formation. In our case small aggregation can be observed in the very small wave vector range of SANS measurement, but the total amount of protein involved in such phenomena is certainly small since no stretching is observed in the intermediate scattering function measured by NSE. The protein charge $|Z_p| \simeq 2$ and is not concentration dependent. The question whether the structure of water (or solvent in general) can be neglected still remains an open question in particular with respect to the possible structure induced by counter ions clouds around the protein. Indirectly the structure of water is important due to its effect on the dielectric constant. We neglect both effects, and suppose that on this lengths scales the medium can be considered homogeneous. It was suggested that the DLVO potential is not valid for biological objects [30] but in our special case due to the very small charge carried by the protein and the small salt content this objection is probably not relevant. The self-diffusion coefficient, of an almost spherical protein with radius R, can be measured for $QR \gg 1$ by coherent neutron scattering. The effect of hydrodynamic interaction is observed whatever the length scale which has been studied in this experiment. These indirect interactions are responsible for the slowing down of the self-diffusion coefficient D_s, since the structure factor in the wave-vector range were it can be measured is $S(Q) \simeq 1$. The hydrodynamic factor $H(Q)$ is wave vector dependent and seems to oscillate in phase with the structure factor, as measured for the concentration up to $\Phi \simeq 0.4$. For wave vectors below a certain value, collective behaviour due to interactions start to dominate with a speed up of the diffusion. In this Q range we probe the Fourier components of concentration fluctuations $\delta\Phi_q$ of wavelength bigger than the mean intermolecular distances. These decay faster due to collective behaviour. The collective diffusion coefficient is generally assumed to be

$$D_c = \frac{1}{f}\frac{\partial \pi}{\partial C}, \tag{35}$$

where f is the solvent friction coefficient and $\partial\pi/\partial C$ the reciprocal osmotic compressibility. The later term acts as a force which tends to relax the concentration fluctuations. Nevertheless due to limited wave vector range of the experiment we were not able to measure the collective diffusion observed by QLS.

Acknowledgements

We would like to thank D. Lairez and A. Brulet from LLB, for respective help in conducting SANS measurements on PACE and spin-echo measurements on MESS.

References

[1] J.B. Wittenberg, J. Biol. Chem. 241 (1966) 104.
[2] P. Doherty, G.B. Benedek, J. Chem. Phys. 61 (1975) 5426.
[3] M.B. Weissman, R.C. Pan, B.R. Ware, J. Chem. Phys. 70 (1979) 2897.
[4] M.B. Weissman, J. Marque, J. Chem. Phys. 73 (1980) 3999.
[5] B. Jacrot, Rep. Prog. Phys. 39 (1976) 911.
[6] R.J. Millero, R. Dexter, E. Hoff, J. Chem. Eng. Data 16 (1971) 86.
[7] J.S. Higgins, H.C. Benoît, in: Gen. Ed. S.W. Lovesey, E.W.J. Mitchell (Eds.), Polymer and Neutron Scattering, Oxford Series on Neutron Scattering in Condensed Matter, vol. 8.
[8] J.B. Hayter, J. Penfold, Mol. Phys. 42 (1981) 109.
[9] L. Belloni, J. Chem. Phys. 85 (1986) 519.
[10] F. Mezei, Z. Physik B 255 (1980) 146.
[11] F. Meizei (Ed.), Neutron Spin-Echo, Lecture Notes in Physics, Springer, Berlin, 1980.
[12] J. Behlke, I. Wandt, Acta Biol. Med. Germ. 31 (1973) 383.
[13] J.P. Cotton, in: P. Lindner, T. Zemb (Eds.), Neutron, X-Ray and Light Scattering, Elsevier, Amsterdam, 1991, p. 3.
[14] R. Gähler, R. Golub, Z. Physik B – Condens. Matter 65 (1987) 269.
[15] R. Golub, R. Gähler, Phys. Lett. A 123 (1987) 43.
[16] K. Ibel, H.B. Stuhrmann, J. Mol. Biol. 93 (1975) 255.
[17] C. Loupiac, M. Bonetti, S. Pin, P. Calmettes, Eur. J. Biochem. 269 (2002) 4731.
[18] S. Longeville, W. Doster, M. Diehl, R. Gähler, W. Petry, in: F. Mezei, C. Pappas, T. Gutberlet (Eds.), Neutron Spin

Echo Spectroscopy, Basic Trends and Applications, Lecture Notes in Physics, vol. 601, Springer, Berlin, 2002.
[19] P.G. de Gennes, Physica 25 (1959) 825.
[20] G.H. Vineyard, Phys. Rev. 110 (1958) 999.
[21] P.N. Segré, O.P. Behrend, P.N. Pusey, Phys. Rev. E 52 (1995) 5070.
[22] V. Riveros-Moreno, J.B. Wittenberg, J. Biol. Chem. 247 (1972) 895.
[23] B.J. Ackerson, J. Chem. Phys. 64 (1976) 242.
[24] P.N. Pusey, J. Phys. A: Math. Gen. 8 (1975) 1433.
[25] P.N. Pusey, in: J.P. Hansen, D. Levesque, J. Zinn-Justin (Eds.), Liquids, Freezing and the Glass Transition, Elsevier, Amsterdam, 1991 (Chapter 10).
[26] Y.S. Oh, C.H. Johnson, J. Chem. Phys. 74 (1981) 2717.
[27] R.S. Hall, C.H. Johnson, J. Chem. Phys. 72 (1980) 4251.
[28] S. Krueger, R. Nossal, Biophys. J. 53 (1988) 97.
[29] S. Krueger, S.H. Chen, J. Hofrichter, R. Nossal, Biophys. J. 58 (1990) 745.
[30] M. Bostrom, D.R.M. Williams, B.W. Ninham, Phys. Rev. Lett. 87 (2001) 168103.